Research Square

Preprints are preliminary reports that have not undergone peer review.
They should not be considered conclusive, used to inform clinical practice,
or referenced by the media as validated information.

Vegetation changes in Central Asia: uncovering their impacts on regional and Asian climate systems

Ahyeong Im
Kyung Hee University
Minjoo Kim
Kyung Hee University
Eungul Lee
eungul.lee@khu.ac.kr

Kyung Hee University

Research Article

Keywords: Land cover and land use, Vegetation changes, Land-atmosphere interactions, Asian jet, Causal analysis, Central Asia

Posted Date: November 17th, 2026

DOI: https://doi.org/10.21203/rs.3.rs-11396697/v1

License: This work is licensed under a Creative Commons Attribution 4.0 International License.
Read Full License

Additional Declarations: No competing interests reported.

Vegetation changes in Central Asia: uncovering their impacts on regional and Asian climate systems

Ahyeong Im [a], Minjoo Kim [a], and Eungul Lee [a, b]

[a] *Department of Climate-Social Science Convergence, Kyung Hee University, Seoul 02447, Republic of Korea*

[b] *Department of Geography, Kyung Hee University, Seoul 02447, Republic of Korea*

Corresponding author: *Eungul Lee*, eungul.lee@khu.ac.kr

ORCID ID: Ahyeong Im (0000-0003-3717-7013), Minjoo Kim (0009-0006-4746-1113), and Eungul Lee (0000-0002-1887-1870)

ABSTRACT

Central Asia is one of the most arid regions in the world and is highly vulnerable to climate change. This region has undergone extensive land cover and land use (LCLU) changes over several decades, including the expansion of irrigation during the Soviet era and the subsequent abandonment of cropland after the post-Soviet disintegration. This widespread abandonment represented one of the most extensive LCLU changes in the Northern Hemisphere during the 20th century. Changes in land cover can alter the energy, moisture, and momentum balances, thereby influencing atmospheric processes. However, compared to other Asian regions, significantly fewer studies have examined the impacts of LCLU changes on climate in Central Asia. This study explored the relationships between vegetation changes in Central Asia and climate during the boreal summer through the empirical association (correlation and regression analyses) and causality (Granger-causality test, Convergent Cross Mapping, and Structural Equation Modeling) analyses, supported by the model datasets (multi-model ensemble means). The results showed that a reduction in vegetation significantly decreased latent heat flux, causing sensible heat flux to dominate land-atmosphere energy exchanges and consequently elevating tropospheric temperatures. This thermal expansion in the troposphere elevated the geopotential height, generating an anomalous anticyclonic circulation supported by a significant negative vorticity anomaly in the upper troposphere. The anticyclonic anomaly induced an easterly wind anomaly that counteracted the prevailing wind, thereby weakening the westerly upper-level jet (i.e., the Asian jet) over Central Asia. Our study highlights that vegetation changes in Central Asia can significantly affect not only the regional climate but also the Asian atmospheric circulation.

Keywords: Land cover and land use, Vegetation changes, Land-atmosphere interactions, Asian jet, Causal analysis, Central Asia

1. Introduction

Central Asia is one of the driest regions in the world, accounting for approximately one-tenth of Earth's total drylands (Middleton and Thomas 1997). The region experiences significant diurnal and seasonal temperature variations and has a semi-arid and arid climate due to persistent moisture deficits and low relative humidity (Li *et al* 2015). This makes Central Asia highly sensitive and vulnerable to climate change, with temperatures increasing approximately twice as rapidly as the global average (Masson-Delmotte *et al* 2018) and extreme heat significantly increasing (Pörtner *et al* 2022). However, compared to other regions in Asia such as East Asia, Southeast Asia, and South Asia, relatively less attention has been paid to the impacts of climate change in Central Asia, with fewer studies available (Mirzabaev 2023; Vakulchuk *et al* 2023).

Over the past few decades, Central Asia has experienced extensive changes in land cover and land use (LCLU). For example, under the influence of the Soviet Union from the 1930s to 1991, irrigated agriculture expanded significantly to alleviate food shortages (Saiko and Zonn 2000; Kariyeva and van Leeuwen 2012). As a result, irrigated agricultural lands increased by 70%, with 45 million hectares of grassland converted into cropland, half of which was in Russia and Kazakhstan (McCauley 2016). However, after the disintegration of the Soviet Union and its agricultural system in 1991, up to 20 million hectares of large-scale croplands were abandoned (FAO 2004). Consequently, between 1990 and 2007, approximately 45.5 million hectares of cropland were abandoned in Russia (Lyuri *et al* 2010) and 12.9 million in Kazakhstan (Morgounov and Trethowan 2008). Given that the total cropland area in Russia and Kazakhstan was 141.8 million hectares in 1990, more than 40% of this cropland was abandoned within a short period (Kurganova *et al* 2015). Indeed, this phenomenon in Central Asia represented the most widespread and abrupt LCLU changes in the Northern Hemisphere during the twentieth century (Henebry 2009; Kurganova *et al* 2015; Lejeune *et al* 2018).

Therefore, Central Asia warrants a separate investigation because of the unique combination of its climatic characteristics and land cover history. As one of the world's largest arid and semi-arid regions, Central Asia is highly vulnerable to climate change owing to limited water availability, strong land–atmosphere coupling, and pronounced hydroclimatic variability (IPCC 2022; Lioubimtseva and Henebry 2009). At the same time, the region has experienced one of the most extensive episodes of anthropogenic LCLU change in the Northern Hemisphere, including widespread cropland abandonment following

the disintegration of the Soviet Union (de Beurs and Henebry 2004; Lioubimtseva and Henebry 2009). The coexistence of exceptional regional climate vulnerability and large-scale historical vegetation changes makes Central Asia an ideal natural laboratory for investigating how LCLU changes influence regional climate and large-scale atmospheric processes.

Widespread LCLU changes have affected Earth's systems since the late twentieth century (Bonan *et al* 1992; Foley *et al* 2005; Pielke Sr 2005; Turner *et al* 2007; Pongratz *et al* 2021). Land covers alter energy, moisture, and momentum balances, thereby influencing atmospheric dynamics and thermodynamics (Seneviratne *et al* 2006; Bonan 2008; Perugini *et al* 2017). This can lead to changes not only in regional climates (Diffenbaugh 2009; Middel *et al* 2012; Duveiller *et al* 2020; Ortiz-Oliveros *et al* 2022), including Europe and Central Asia (Davin *et al* 2020; de Noblet-Ducoudré *et al* 2012), but also in global climate systems (Lee *et al* 2011; Lawrence *et al* 2012). Accordingly, despite uncertainties regarding the magnitude of their impacts, LCLU changes are recognized as important climate forcings at local, regional, and global scales (Chase *et al* 2000; Mahmood *et al* 2014; Perugini *et al* 2017; Pongratz *et al* 2021). Numerous studies have examined the impact of LCLU changes on climate systems across various regions (Pitman *et al* 2009), including East Asia (Cao *et al* 2021; Yadav *et al* 2022; Fan *et al* 2025), South Asia (Biggs *et al* 2008; Rajagopalan and Molnar 2013), North America (Ozdogan *et al* 2010; Xian *et al* 2020), and Africa (Lee *et al* 2015). For example, Yadav *et al* (2022) analyzed that changing vegetation on the western Tibetan Plateau can alter temperatures near the surface and in the upper atmosphere through positive physical linkages among vegetation cover, surface energy flux, and temperatures. Compared to other regions, significantly fewer studies have investigated the impacts of LCLU changes on climate in Central Asia. Additionally, studies on the effects of LCLU changes on the regional climate in Central Asia have mainly focused on the surface climate (e.g., Yuan *et al* 2017), whereas the impacts on mid- and upper-level atmospheric climates have only been explored through model-based studies (e.g., Lee *et al* 2011). Considering the unique combination of extensive historical LCLU changes, the climate vulnerability of this arid region, and the limited observational evidence available, a comprehensive investigation of vegetation–climate interactions in Central Asia is needed.

The novelty of this study is threefold. First, unlike previous studies that mainly relied on numerical simulations, we provide an observation-based empirical assessment of how historical vegetation changes influence regional climate in Central Asia. Second, we extend the analysis beyond surface climate to demonstrate how vegetation changes can influence the

106 troposphere and the upper-level atmospheric circulation. Third, we integrate complementary
107 association analyses (correlation and regression analyses), causality analyses (Granger-
108 causality test, Convergent Cross Mapping, and Structural Equation Modeling), and the
109 analyzed model datasets (simulations from the Coupled Model Intercomparison Project Phase
110 6 (CMIP6) and the Land Use Model Intercomparison Project (LUMIP)) to provide robust
111 evidence for the climatic impacts of vegetation changes.

112 Therefore, we aimed to quantitatively assess the impacts of LCLU changes on the
113 climate system in Central Asia through association and causality analyses using multiple
114 datasets of observation-based (i.e., satellite-based vegetation and climate reanalysis datasets),
115 supported by the multi-model ensemble (MME) datasets. As an empirical study, we provide
116 insights into how changes in the LCLU in Central Asia can influence not only the regional
117 climate but also the Asian climate systems.

2. Data and methods

2.1. Data

2.1.1. Vegetation data

To investigate the overall vegetation changes in Central Asia and surrounding regions (20–70°N and 20–100°E), we used AVHRR Global Inventory Modeling and Mapping Studies (GIMMS) Normalized Difference Vegetation Index (NDVI) data (Pinzon *et al* 2023). The study period was set to 1991–2022, considering data availability and the timing of a specific historical event (i.e., disintegration of the Soviet Union) that could significantly affect LCLU in the region. Over the past two decades, NDVI has been a reliable indicator for detecting vegetation cover and variability at regional, continental, and global scales (Olusegun and Adeyewa 2013; Schmidt *et al* 2014; Xu *et al* 2016). These data have a spatial resolution of 8 km and provide two values per month for a composite period of 14–16 days. In this study, we calculated annual and seasonal NDVI means for the study period. To compare the vegetation changes with changes in agricultural land use, the land cover maps have been utilized to examine the percentage change of annual cropland fraction using the GLASS-GLC (Liu et al., 2020). The results of annual cropland fraction and its trend are shown in the Supplementary information (figure S2).

2.1.2. Climate data

All atmospheric variables from 1991 to 2022 were retrieved from the European Centre for Medium-Range Weather Forecasts (ECMWF) Reanalysis (ERA5). Surface climate variables from ERA5-Land with a spatial resolution of 0.1° (Muñoz-Sabater *et al* 2021) were used to examine the impacts of vegetation changes on the near-surface climate using latent and sensible heat fluxes, 2m specific humidity, and 2m temperature. Additionally, the surface energy budget and hydrological variables were utilized, including surface net solar radiation, surface solar radiation downwards, and surface net thermal radiation as energy budget variables, and root zone soil water (~ 100 cm), total evaporation, and total precipitation as hydrological variables. 2m specific humidity was calculated using 2m dew point temperature and surface pressure based on the following expressions (ECMWF 2016):

$$e = 6.112 * \exp\left\{\frac{17.67*Td}{Td+243.5}\right\} \quad (1)$$

$$q = \frac{0.622*e}{ps-(0.378*e)} \quad (2)$$

where e is the actual vapor pressure, Td is the 2m dew point temperature, q is the specific humidity, and ps is the surface pressure.

To examine the influence of vegetation changes on mid- and upper-level atmospheric conditions and circulations, we used temperature, geopotential height, vorticity, and u-wind data from the ERA5-Pressure. ERA5-Pressure data were produced at multiple pressure levels (from 1000 to 1 hPa) with a spatial resolution of 0.25°. In this study, we calculated the boreal summer (June to August, JJA) average using the ERA5 monthly data for each variable.

2.1.3. Model data

To confirm the observed climate impact of LCLU changes in the GIMMS NDVI dataset, we utilized the MME datasets from CMIP6 (Eyring *et al* 2016) and LUMIP (Lawrence *et al* 2016). We have estimated the simulated changes in Leaf Area Index (LAI) and near-surface climate variables based on the MME means using the 10 GCMs, including NorESM2-LM, ACCESS-ESM1-5, IPSL-CM6A-LR, BCC-CSM2-MR, CanESM5, CMCC-ESM2, MPI-ESM1-2-LR, EC-Earth3-Veg, GFDL-ESM4, and CESM2. Particularly, we compared the results from two MME simulation datasets: the *historical* simulation from CMIP6 and the *hist-noLu* simulation from LUMIP. *historical* simulation spans the period from 1850 to 2014 and is driven by anthropogenic (e.g., LCLU changes and greenhouse gas emissions) and natural forcings (e.g., volcanic forcings). *hist-noLu* is identical to the *historical*, except that LCLU is maintained at 1850 levels (Luo *et al* 2024). Accordingly, the difference between the *historical* and *hist-noLu* simulations primarily represents the biophysical impacts of historical human-induced LCLU changes, because both experiments share the same natural and anthropogenic climate forcings except for the prescribed LCLU conditions. This experimental design enables the isolation of the climatic effects of historical LCLU changes while minimizing the influence of other external forcings.

For the 1991–2014 period, we used simulated LAI data to represent LCLU conditions. LAI is a crucial variable in Earth System Models (ESMs) that controls land-

atmosphere interactions, including surface energy balance and the hydrological cycle (Park and Jeong 2021). Since NDVI is not included in CMIP6 model datasets, the simulated LAI was used as an alternative indicator. Although NDVI and LAI are different vegetation indicators, both are widely used to characterize vegetation density and greenness and generally exhibit similar responses to vegetation changes (Myneni and Williams 1994). Because LAI is directly simulated in the ESMs whereas NDVI is not available as a standard model output, simulated LAI was used as the model counterpart to the observed NDVI. Nevertheless, NDVI and LAI differ in their physical definitions and sensitivities to vegetation structure and canopy conditions, particularly in densely vegetated regions where NDVI may become saturated while LAI continues to increase (Myneni and Williams 1994; Kang *et al* 2021). Therefore, the comparison between observed NDVI and simulated LAI should be interpreted as an evaluation of the consistency of large-scale vegetation changes rather than as a direct one-to-one comparison between the two variables.

Additionally, to examine the simulated impacts of vegetation (i.e., LAI) changes on the near-surface climate over Central Asia from 1991 to 2014, we used latent and sensible heat fluxes, 2m temperature, and 2m specific humidity from the *historical* simulations of MME. In this study, we calculated the JJA average using the monthly data for each variable to be consistent with the observed analyses. The simulated results of MME are shown in the Supplementary information of figures S3 (LAI changes), S6 (Correlation analysis), and S7 (Linear regression analysis).

2.2. Statistical methods

2.2.1. Spatiotemporal changes in vegetation and surface climate variables

To investigate the spatiotemporal changes in vegetation and near-surface climate variables in Central Asia and surrounding regions (20–70°N and 20–100°E), we performed linear regression analyses. We focused particularly on JJA, when vegetation activity is most vigorous in arid regions. The simple linear regression model used in this study is as follows:

$$Y = aX + b + e \quad (3)$$

where parameters *a* and *b* are the regression coefficients estimated by the least squares method, and *e* represents the regression residual. Here, *a* indicates the change in *Y* variables (i.e., observed NDVI, simulated LAI, and near-surface climate variables) over time *X* (i.e., year) for both observation-based and model datasets, respectively. Only grid cells that were statistically significant at the 5% level in both analyses are shown on the map.

Additionally, we performed a non-parametric Mann–Kendall (MK) test to justify the assumed linearity in the trend analyses (Mann 1945; Kendall 1948). The MK test is distribution-free and robust to outliers in time series, making it widely used for trend detection in hydrological and climate time series (Araghi *et al* 2015; Alsaaran and Alghamdi 2022; Im *et al* 2026). We also used the Theil-Sen regression because the MK test cannot estimate the magnitude of the trend (Sen 1968). If the null hypothesis of no monotonic trend in the time series was rejected by the MK test, the magnitude of the trend was quantified using Sen's slope. Significance tests for non-parametric analyses were conducted at three different levels (1%, 5%, and 10%) to verify the robustness of the significant patterns (Siderius *et al* 2014; Im *et al* 2026). As the statistically significant patterns of analyses at the 5% significance level were consistent with those of the parametric analyses, we present the non-parametric results in the Supplementary information (figures S1 and S4).

2.2.2. Relationships between vegetation and surface climate variables

We performed a correlation analysis between vegetation (GIMMS NDVI and simulated LAI) and surface climate variables using both observation-based (ERA5-Land) and model datasets (MME means) for each grid cell to investigate the relationship between vegetation and near-surface climate in Central Asia. Additionally, to quantify the magnitude of change in each climate variable over a unit change in the vegetation variable, we conducted a linear regression analysis. The independent variable (*X*) was the vegetation variable, and the dependent variable (*Y*) was the surface climate. Only grid cells that were statistically significant at the 5% level were observed in both analyses.

To verify the causal relationships identified through association analyses, we performed a Granger-causality test (Granger 1969) for linear causality and Convergent Cross Mapping (CCM; Sugihara *et al* 2012) for non-linear causality. For these analyses, we used the area-averaged time series of grids representing a significant decrease in NDVI within the study region (40–52°N and 40–70°E) during JJA. The Granger-causality test states that if

past data on the time series variable X are more useful for explaining the future state of the time series variable Y than the past data on Y itself, then X is said to have a causal relationship with Y. This test involves comparing two regression models: one that regresses Y only on its lagged values, and another that regresses Y on both its lagged values and the lagged values of X. If the regression model including X shows a significant improvement in explaining the variability of Y compared to the model without X, it is said to X does Granger-cause Y. Next, the F-test statistic was used to test for statistically significant differences between the two regression models. Because it is a two-way interaction, the same reasoning applies to inverse Granger causal relationships.

To clarify the causal associations in the complex natural system, we conducted the CCM. The shadow manifolds (Mx and My) were reconstructed from the time series of each variable using time-delay embedding, in which each state of the system is represented by a vector composed of lagged observations. According to Takens' embedding theorem (Takens 1981), the reconstructed manifold preserves the underlying dynamics of the original system and enables causal information shared between variables to be recovered (Sugihara *et al* 2012). Given points in the manifold My of a variable in the $Y = f(X, Y)$ system, the corresponding points in the manifold Mx of another variable (i.e., points at the same time t) can be found. If X is a cause for Y, information about X is embedded in Y, allowing X to be predicted from Y. Since the interaction is bidirectional, the same reasoning applies to the inverse causality. To assess causality accuracy, we calculated the population *Pearson* correlation coefficients (ρ) between observed and CCM-predicted values, where increasing ρ with longer time series indicates improved estimation skill and reduced error. Therefore, convergence of the cross-mapping skill (ρ) with increasing time-series length was interpreted as evidence of a causal relationship, whereas little or no improvement in ρ indicated weak or absent causal influence (Sugihara *et al* 2012; Ye *et al* 2015).

Furthermore, to investigate the thermodynamic processes by which vegetation changes influence surface climate, we applied Structural Equation Modeling (SEM) to estimate causal relationships through direct and indirect pathways (Streiner 2005). We hypothesized that vegetation reduction in arid Central Asia alters surface energy partitioning— by decreasing latent heat and increasing sensible heat fluxes—which reduces evaporative fraction and raises surface temperatures. To address the multicollinearity issue in using latent and sensible heat fluxes in SEM and to reflect the moisture-sensitive characteristics of the arid climate, we calculated and utilized the evaporative fraction, defined

as the ratio of latent heat to the sum of latent and sensible heat fluxes. Path coefficients were calculated using maximum likelihood estimation. To assess model performance, we calculated fit indices including the comparative fit index (CFI), goodness of fit index (GFI), and root mean square error of approximation (RMSEA). Model fit was assessed against standard criteria (CFI ≥ 0.95, GFI ≥ 0.95, and RMSEA ≤ 0.10) (Qing *et al* 2025).

2.2.3. Relationships between vegetation and atmospheric circulation

We performed vertical cross sections of NDVI correlation with temperature and geopotential height (from 1000 to 100 hPa) to explore the relationships between vegetation and mid- and upper-level climate variables in Central Asia using meridionally averaged values over European Russia and northwestern Kazakhstan (40-52°N). To examine the atmospheric conditions associated with reduced vegetation activity, we also analyzed vertical cross sections of the composite differences in temperature and geopotential height (from 1000 to 100 hPa) between the years with high and low NDVI. We calculated the difference in atmospheric variables between the six years of the lowest JJA NDVI and the six years of the highest JJA NDVI. These selected years corresponded to the top and bottom 20% of the study period (1991-2022). The years with the highest NDVI (top 20%) were 1993, 1997, 1992, 2000, 1994, and 2003, whereas those with the lowest NDVI (bottom 20%) were 2021, 2020, 2019, 2018, 2012, and 2010. To investigate the changes in Asian atmospheric circulation associated with variations in vegetation in Central Asia, we conducted a composite difference analysis of upper-level (200 hPa) vorticity and *u*-wind. As mentioned previously, we calculated the difference in vorticity and *u*-wind between the six years of the lowest JJA NDVI and the six years of the highest JJA NDVI. Only the statistically significant regions at the 5% and 10% levels were contoured in the results.

Additionally, we applied the detrended analyses to evaluate the effect of land forcing on the relationship between vegetation and climate variables by eliminating trends such as global warming (Supplementary information of figure S5). Also, the upper-level atmospheric conditions over the study regions in Asia are linked to large-scale climate variability such as the El Niño-Southern Oscillation (ENSO). To suppress the ENSO forcing, we statistically removed the linear trends of ENSO using the Oceanic Niño Index (ONI) (NOAA CPC n.d.; Glantz and Ramirez 2020) by subtracting the slope coefficient calculated using the least squares method of linear regression from the vegetation and climate variables (Hurley and

306 Boos 2013; Kim *et al* 2025). As the statistically significant spatial patterns of analyses at the
307 5% significance level were consistent with those of the detrended and ENSO-removed
308 analyses, we show the results without detrended and ENSO-removed in the main sections.
309 The results of detrended and ENSO-removed analyses of atmospheric variables are shown in
310 the Supplementary information (figure S8).

3. Results

3.1. Spatiotemporal changes in vegetation and surface climate variables in Central Asia

We examined changes in the annual and seasonally averaged NDVI in Central Asia and its surrounding regions (20–70°N, 20–100°E) (see dashed box in figure 1(a)) from 1991 to 2022 (figure 1). The highest rates of increase, exceeding 20% per 32 years, were observed in northwestern Russia and western India. High-latitude regions, including northwestern Russia, have been warming faster than the global average (Francis and Vavrus 2015; Xu *et al* 2020). Increasing temperatures promote vegetation growth (Forbes *et al* 2010; Zhu *et al* 2016; Liu *et al* 2020). Thus, the rapid increase in the NDVI shown in figure 1 could be related to the rapid warming of the region (Hess and Tasa 2019), which could extend the growing period and expand the habitable areas for vegetation. The increase in the NDVI in western India was associated with cropland expansion. According to previous studies, croplands are generally the dominant land cover type across India and have significantly increased, particularly in western India since the 1980s (Liu *et al* 2021; He *et al* 2022), which is consistent with the changes in NDVI identified in this study. In contrast, the highest rate of decrease was observed in European Russia and Kazakhstan, exceeding 15% per 32 years. The decrease in NDVI, which intensified in JJA, continued into SON (September to November) in European Russia and northwestern Kazakhstan (figures 1(e) and 1(f)). The spatial patterns of non-parametric analysis at three different levels of 1%, 5%, and 10% were almost consistent with those of parametric analysis (5% level shown in figure S1 and 1% and 10% are not shown here). Accordingly, the Central Asian region of European Russia and northwestern Kazakhstan (40–52°N, 40–70°E) was selected as the study region (see solid box in figure 1(a)). As a temporal period, we focused on the boreal summer (JJA), when vegetation activity is most significant in arid regions. Additionally, the vegetation changes were consistent with the significant decreasing trends of annual cropland fraction in Eastern Europe and European Russia based on the GLASS-GLC from 1991 to 2015 (figure S2).

An analysis of model datasets was performed to validate these observation-based results. The *historical* experiment data, which incorporates the impacts of human-induced LCLU changes, showed a significantly different change in vegetation in the regions of Eastern Europe and European Russia, compared to the *hist-noLu* experiment (figure S3). The spatial patterns of decreasing LAI trend during 1991-2014 simulated by the 10 GCM MME

means (figure S3(c)) generally agreed with the decreasing NDVI trends during 1991-2022 in observation-based data by capturing the substantial vegetation decline in European Russia since 1991.

Over the same period, the study region exhibited decreases of over 0.5 W m^{-2} per year in latent heat flux (figure 2(a)) and 0.0003 g kg^{-1} per year in 2m specific humidity (figure 2(c)). In contrast, sensible heat flux and 2m temperature increased by more than 0.5 W m^{-2} and 0.07 °C per year, respectively (figures 2(b) and 2(d)). The patterns of the non-parametric analysis were generally consistent with those of the parametric analysis at three different levels of 1%, 5%, and 10% (5% level shown in figure S4 and 1% and 10% are not shown here). Additionally, the regression trend analyses with the surface energy budget and hydrological variables were consistent with those of surface heat fluxes, 2m specific humidity, and 2m temperature. The increasing trends in the variables of the surface energy budget were significant in European Russia and northwestern Kazakhstan (figures 3(a), 3(b), and 3(c)), while the significant decrease in hydrological variables was distinct in the regions (figures 3(d), 3(e), and 3(f)).

3.2. Relationships between vegetation and surface climate variables in Central Asia

Correlation and regression analyses

To investigate whether there were associations between the interannual variability of vegetation and surface climate in Central Asia, correlation (figures 4 and 5) and linear regression (figure 6) analyses of NDVI with surface climate variables were performed for 32 years. In European Russia and northwestern Kazakhstan, latent heat flux and 2m specific humidity were positively correlated with NDVI ($r > 0.4$) (figures 4(a) and 4(c)), but sensible heat flux and 2m temperature showed a negative correlation with NDVI ($r < -0.4$) (figures 4(b) and 4(d)). These results indicate that in European Russia and northwestern Kazakhstan, a decrease in NDVI was associated with a decrease in latent heat flux and 2m specific humidity, and an increase in sensible heat flux and 2m temperature. The spatial patterns of the correlations were generally consistent with those of the detrended correlation analysis (figure S5). Additionally, the correlation analyses of NDVI with the surface energy budget (i.e., surface solar radiation downwards and surface net thermal radiation) and hydrological (i.e., root zone soil water, total evaporation, and total precipitation) variables were conducted. The negative correlations in the variables of the surface energy budget were significant in

European Russia and northwestern Kazakhstan (figures 5(a), 5(b), and 5(c)), while the significant positive associations between NDVI and hydrological variables were identified (figures 5(d), 5(e), and 5(f)). The consistent results with and without trends and the additional energy budget and hydrological variables supported the idea that vegetation change had a significant forcing on near-surface heat and moisture conditions in the Central Asian region.

While the correlation analysis (see figure 4) identifies the spatial patterns and direction of the vegetation–climate relationship, the linear regression analysis (figure 6) further quantifies the magnitude of the climate response associated with vegetation changes. The results of the linear regression showed that, in European Russia and northwestern Kazakhstan, as NDVI decreased by 0.1, the latent heat flux and 2m specific humidity decreased by more than 5 W m^{-2} and 0.004 g kg^{-1}, respectively (figures 6(a) and 6(c)). Contrastingly, as NDVI decreased by 0.1, the sensible heat flux and 2m temperature increased by more than 5 W m^{-2} and 1°C, respectively (figures 6(b) and 6(d)). These results demonstrate the sensitivity of the near-surface climate variables to changes in vegetation, complementing the spatial relationships identified by the correlation analysis.

Additionally, the simulated spatial patterns of the correlation and regression between LAI and surface climate variables from the *historical* simulations of MME means were mostly consistent with the observation-based results (figures S6 and S7). In Eastern Europe and European Russia, LAI was positively correlated with latent heat flux from *historical* (figure S6(a)). Conversely, there was a negative correlation of LAI with sensible heat flux (figure S6(b)) and 2m temperature (figure S6(d)), respectively. Additionally, the linear regression analysis of *historical* showed that as LAI decreased by 1, the latent heat flux decreased by more than 6 W m^{-2} in Eastern Europe and European Russia (figure S7(a)). In contrast, as LAI decreased by 1, the sensible heat flux and 2m temperature increased by more than 12 W m^{-2} and 1.6°C, respectively, in the regions (figures S7(b) and S7(d)).

Causality analyses

The association analyses with correlation and linear regression did not demonstrate causal relationships; therefore, we performed a Granger-causality analysis to examine the causal association between vegetation and surface climate in the study region (table 1). According to the results, NDVI does Granger cause all four surface climate variables, except for sensible heat flux (p-value = 0.096, 0.052, and 0.004 for 2m temperature, latent heat flux,

and 2m specific humidity, respectively) (table 1(a)). However, all the climate variables do not Granger cause NDVI ($p > 0.1$) (table 1(b)). Particularly, latent heat flux does Granger cause 2m specific humidity and 2m temperature ($p < 0.1$) (table 1(c)), but all the climate variables do not Granger cause latent heat flux ($p > 0.1$) (table 1(d)).

To ensure the robustness of these findings, we performed CCM as a non-linear causality test (upper panel in figure 7). The black lines are the correlation coefficients indicating that NDVI causes latent heat flux (figure 7(a)), sensible heat flux (figure 7(b)), 2m specific humidity (figure 7(c)), and 2m temperature (figure 7(d)), respectively, and the red lines are the correlation coefficients indicating vice versa. The correlation coefficients (ρ) represent the *Pearson* correlation between the observed and predicted variables by the information involved in another variable. The results demonstrated that all ρ values, which indicate the causal effect of NDVI on surface climate, were statistically significant at the 1% level (ρ = 0.412, 0.394, 0.466, and 0.392 for latent heat flux, sensible heat flux, 2m specific humidity, and 2m temperature, respectively). Through the non-linear causality analysis of this complex coupled natural system, it was demonstrated that vegetation acts as a causal driver for surface climate variables.

We then performed SEM to explore the thermodynamic processes underlying the climate responses to vegetation changes (lower panel in figure 7). Our findings indicated that a reduction in NDVI significantly decreased latent heat flux and simultaneously amplified sensible heat flux, with path coefficients of 0.90 and -0.76, respectively ($p < 0.01$). This shift in surface energy partitioning induced a substantial reduction in evaporative fraction. The suppressed evaporative fraction subsequently led to an increase in near-surface temperature with a path coefficient of -0.68 ($p < 0.01$). Ultimately, this pathway demonstrated how a decrease in vegetation exacerbated regional warming through altered surface energy balances within the moisture-sensitive arid environment of Central Asia.

3.3. Relationships between vegetation and atmospheric circulation in Central Asia

To explore the relationships between vegetation and tropospheric climates in Central Asia, we performed vertical cross sections of both the correlation of NDVI with tropospheric temperature and geopotential height, and the composite differences of these variables between low and high NDVI years (figure 8). From near the surface to the upper atmosphere (1000–200 hPa), there were continuous negative relationships between NDVI and

439 temperature, with distinct warming anomalies at lower levels, which were directly affected by
440 vegetation changes (figures 8(a) and 8(b)). Correspondingly, negative associations between
441 NDVI and geopotential height were observed in the entire troposphere over the study region
442 owing to the thermal expansion of the atmosphere (figures 8(c) and 8(d)). Consistently, the
443 significant negative associations of NDVI with the tropospheric thermal and dynamic
444 variables above European Russia and northwestern Kazakhstan were identified in the
445 detrended analysis (figure S8 in the upper panel) and the ENSO-removed analysis (figure S8
446 in the lower panel). These consistent results demonstrate that the warming effect due to
447 decreased summer NDVI can extend from near the surface to the upper atmosphere in Central
448 Asia.

449 To investigate whether significant tropospheric thermal perturbations in Central Asia
450 can impact atmospheric circulation in Asia, the composite differences in vorticity with the
451 wind vector and *u*-wind in the upper atmosphere at 200 hPa were examined by comparing
452 their climatological patterns (32-year averages) (figure 9). In Central Asia, the climatology of
453 the 200 hPa vorticity showed positive values in the region above 40°N but negative values
454 below 40°N (figure 9(a)). The westerlies from the positive and negative vorticities resulted in
455 the strongest westerly winds of up to 30m s^{-1} (i.e., the Asian jet) around 35–45°N (figures
456 9(a) and 9(b)). During the years of low NDVI in the study region of European Russia and
457 northwestern Kazakhstan, a significant negative vorticity anomaly and, correspondingly,
458 anomalous anticyclonic circulation were observed in the upper atmosphere over the study
459 region and the surrounding northwestern region (i.e., 45–60°N and 20–60°E; figures 9(c) and
460 9(d)). Additionally, alternating patterns of vorticity anomalies were observed from the
461 forcing region to the East Asian region, with a significant negative-positive-negative
462 anomaly. The anticyclonic anomalous circulation (i.e., the clockwise direction in the
463 Northern Hemisphere), with the center in the 50°N region, caused a significant easterly
464 (westerly) anomaly at 200 hPa in the southern (northern) part of the anomalous circulation
465 around the 45°N (60°N) region (figure 9(e)). Thus, the anomalous easterlies reduced the
466 climatological upper-level westerly winds, significantly weakening the Asian jet over Central
467 Asia.

468 The increase in temperature owing to the decrease in surface vegetation could have
469 led to an increase in temperature from the lower atmosphere to the upper atmosphere. This
470 warming in the troposphere can elevate the geopotential height in the region as the thickness
471 of a layer was increased by thermal expansion (Chase *et al* 2000; Lee *et al* 2011) over the

study region of Central Asia (see geopotential heights in figure 8). An increase in geopotential height could alter the upper-level vorticity and circulation patterns, leading to an anticyclonic anomaly, which results in an easterly wind anomaly in Central Asia. Consequently, the anomalous easterly wind could weaken the westerly upper-level jet over Central Asia.

4. Discussion and conclusions

After the disintegration of the Soviet Union in 1991, the transition from state command to market economics led to the adoption of free-market principles. For instance, the reduction in government regulations, support, and land reforms has induced significant changes across all sectors of the economy, including agricultural land use (Lioubimtseva and Henebry 2009; Prishchepov *et al* 2012). Significant reductions in government subsidies and agricultural support have resulted in large-scale cropland abandonment (Kraemer *et al* 2015; Meyfroidt *et al* 2016). Additionally, rural depopulation and an aging workforce exacerbated geopolitical impacts on agricultural communities as younger populations migrated to urban areas in search of better opportunities (Ioffe *et al* 2004; Meyfroidt *et al* 2016). These changes in the socioeconomic system, driven by specific geopolitical events, might have driven the vegetation changes in European Russia and Kazakhstan identified in this study, thereby exerting a substantial impact on the climate system.

The statistical relationships identified through correlation, regression, and causality analyses, supported by the MME datasets, and the related thermodynamic processes demonstrated that vegetation changes in Central Asia could influence the upper atmospheric circulation across Asia. The impacts on the near-surface climate were particularly significant during the boreal summer in Central Asia, including European Russia and northwestern Kazakhstan. Decreased latent heat flux, along with increased sensible heat flux, resulted in a notable increase in surface temperature. The warming effect extended from the surface to the lower troposphere and reached the upper troposphere. Tropospheric warming caused an increase in the geopotential height due to thermal expansion over Central Asia. These findings suggest that warming induced by a reduction in vegetation could impact atmospheric circulation across Asia through changes in tropospheric height. During periods of lower vegetation activity, a negative vorticity anomaly accompanied by an anomalous anticyclonic circulation was observed in the upper levels over European Russia and northwestern Kazakhstan. The anomalous anticyclonic circulation centered around 50°N generated an easterly wind anomaly at 200 hPa in the southern part of the anomalous circulation (around 45°N) and a westerly wind anomaly in the northern part (around 60°N). These changes weakened the upper-level westerly jet, which climatologically flows at approximately 35–45°N.

These changes in upper atmospheric circulation over Central Asia during summer could significantly impact summer climates in Central Asia and other parts of Asia by

altering monsoon activity and precipitation patterns. For example, changes in the upper-level Asian westerly jet, and thus the South Asian high, could alter precipitation patterns not only in Central Asia but also in the East Asian monsoon region (Wei *et al* 2017). As our results show, atmospheric circulation changes over Asia extend from Central Asia to East Asia through a negative-positive-negative anomaly pattern of upper-level vorticity (see figure 9(c)). Thus, changes in atmospheric circulation caused by vegetation changes can remotely influence the Asian summer monsoon climate.

The empirical relationships identified in this study were generally consistent across multiple statistical approaches, including parametric and non-parametric regressions, detrended and ENSO-removed correlation analyses, linear and nonlinear causality tests, and analyses based on the multi-model ensemble means. These additional analyses increase confidence that the identified relationships are not artifacts of a particular statistical method. Nevertheless, in future studies, dedicated model experiments incorporating human-induced LCLU changes are needed to strengthen the robustness of the inferred impacts of vegetation changes on Asian climate systems. Our empirical study using reanalysis and remotely sensed data, partially supported by model results, provides insights into how vegetation changes in Central Asia can impact the climate systems across Asia.

Acknowledgments

This study is partially funded by the BK21 FOUR program of Graduate School, Kyung Hee University (GS-5-JO-NON-20250787) and the Ministry of Education of the Republic of Korea and the National Research Foundation of Korea (NRF-2025S1A5B5A1901909011).

Conflict of Interest statement

The authors declare no conflicts of interest relevant to this study.

Author's contributions

AI and EL contributed to the study conception and design. Material preparation, data collection, and analysis were led by AI with support from MK. The first draft of the manuscript was written by AI. EL supervised the entire work and reviewed and revised the manuscript. AI, MK and EL read and approved the final manuscript.

Data availability statement

The GIMMS NDVI3g+ are available at https://doi.org/10.3334/ORNLDAAC/2187 as cited in Pinzon et al. (2023). The 10 GCMs of CMIP6 and LUMIP are available at https://aims2.llnl.gov/. The climate data for the ERA5 are available at https://doi.org/10.24381/cds.68d2bb30 for the land, and https://doi.org/10.24381/cds.6860a573 for the pressure level.

References

Alsaaran, N. A., & Alghamdi, A. S. (2022). Precipitation climatology and spatiotemporal trends over the Arabian Peninsula. *Theoretical and Applied Climatology*, 147(3), 1133-1149. https://doi.org/10.1007/s00704-021-03878-5

Araghi, A., Baygi, M. M., Adamowski, J., Malard, J., Nalley, D., & Hasheminia, S. M. (2015). Using wavelet transforms to estimate surface temperature trends and dominant periodicities in Iran based on gridded reanalysis data. *Atmospheric Research,* 155, 52-72. https://doi.org/10.1016/j.atmosres.2014.11.016

Biggs, T. W., Scott, C. A., Gaur, A., Venot, J. P., Chase, T., & Lee, E. (2008). Impacts of irrigation and anthropogenic aerosols on the water balance, heat fluxes, and surface temperature in a river basin. *Water resources research*, 44(12). https://doi.org/10.1029/2008WR006847

Bonan, G. B. (2008). Forests and climate change: forcings, feedbacks, and the climate benefits of forests. science, 320(5882), 1444-1449. https://doi.org/10.1126/science.1155121

Bonan, G., Pollard, D., & Thompson, S. (1992). Effects of boreal forest vegetation on global climate. *Nature,* 359(6397), 716–718. https://doi.org/10.1038/359716a0

Cao, F., Dan, L., Ma, Z., & Gao, T. (2021). The impact of land use and land cover change on regional climate over East Asia during 1980–2010 using a coupled model. *Theoretical and Applied Climatology,* 145, 549-565. https://doi.org/10.1007/s00704-021-03629-6

Chase, T. N., Pielke Sr., R. A., Kittel, T. G. F., Nermani, R. R., & Running, S. W. (2000). Simulated impacts of historical land cover changes on global climate in northern winter. *Climate Dynamics,* 16(2), 93–105. https://doi.org/10.1007/s003820050007

Davin, E. L., Rechid, D., Breil, M., Cardoso, R. M., Coppola, E., Hoffmann, P., ... & Wulfmeyer, V. (2020). Biogeophysical impacts of forestation in Europe: first results from the LUCAS (Land Use and Climate Across Scales) regional climate model intercomparison. Earth System Dynamics, 11(1), 183-200. https://doi.org/10.5194/esd-11-183-2020

de Beurs, K. M., & Henebry, G. M. (2004). Land surface phenology, climatic variation, and institutional change: Analyzing agricultural land cover change in Kazakhstan. Remote

sensing of environment, 89(4), 497-509. https://doi.org/10.1016/j.rse.2003.11.006

de Noblet-Ducoudré, N., Boisier, J. P., Pitman, A., Bonan, G. B., Brovkin, V., Cruz, F., ... & Voldoire, A. (2012). Determining robust impacts of land-use-induced land cover changes on surface climate over North America and Eurasia: results from the first set of LUCID experiments. Journal of Climate, 25(9), 3261-3281. https://doi.org/10.1175/JCLI-D-11-00338.1

Diffenbaugh, N. S. (2009). Influence of modern land cover on the climate of the United States. Climate Dynamics, 33(7), 945-958. https://doi.org/10.1007/s00382-009-0566-z

Duveiller, G., Caporaso, L., Abad-Viñas, R., Perugini, L., Grassi, G., Arneth, A., & Cescatti, A. (2020). Local biophysical effects of land use and land cover change: towards an assessment tool for policy makers. Land use policy, 91, 104382. https://doi.org/10.1016/j.landusepol.2019.104382

European Centre for Medium-Range Weather Forecasts (ECMWF). (2016). *Part IV: Physical processes. IFS Documentation–Cy41r2*. Reading, UK: ECMWF.

Eyring, V., Bony, S., Meehl, G. A., Senior, C. A., Stevens, B., Stouffer, R. J., & Taylor, K. E. (2016). Overview of the Coupled Model Intercomparison Project Phase 6 (CMIP6) experimental design and organization. *Geoscientific Model Development,* 9(5), 1937–1958. https://doi.org/10.5194/gmd-9-1937-2016

Fan, Y., Yang, Z., Lo, M. H., Hur, J., & Im, E. S. (2025). Deciphering the capricious precipitation response: irrigation impact in the North China Plain. *npj climate and atmospheric science,* 8, 211. https://doi.org/10.1038/s41612-025-01063-3

Foley, J. A., Defries, R., Asner, G. P., Barford, C., Bonan, G., Carpenter, S. R., et al. (2005). Global Consequences of Land Use. *Science,* 309(5734), 570-574. https://doi.org/10.1126/science.1111772

Food and Agriculture Organization of the United Nations (FAO). (2004). FAOSTAT statistical database. Retrieved from http://faostat.fao.org

Forbes, B. C., Fauria, M. M., & Zetterberg, P. (2010). Russian Arctic warming and ‘greening’are closely tracked by tundra shrub willows. *Global Change Biology*, 16(5), 1542-1554. https://doi.org/10.1111/j.1365-2486.2009.02047.x

Francis, J. A., & Vavrus, S. J. (2015). Evidence for a wavier jet stream in response to rapid

607 Arctic warming. *Environmental Research Letters*, 10(1), 014005.
608 https://doi.org/10.1088/1748-9326/10/1/014005

609 Glantz, M. H., & Ramirez, I. J. (2020). Reviewing the Oceanic Niño Index (ONI) to enhance
610 societal readiness for El Niño's impacts. International Journal of Disaster Risk Science,
611 11(3), 394-403. https://doi.org/10.1007/s13753-020-00275-w

612 Granger, C. W. (1969). Investigating causal relations by econometric models and cross-
613 spectral methods. *Econometrica: journal of the Econometric Society*, 37(3), 424-438.
614 https://doi.org/10.2307/1912791

615 He, Y., Chipman, J., Siegert, N., & Mankin, J. S. (2022). Rapid land-cover and land-use
616 change in the Indo-Malaysian region over the last thirty-four years based on AVHRR
617 NDVI data. *Annals of the American Association of Geographers*, 112(8), 2131-2151.
618 https://doi.org/10.1080/24694452.2022.2077168

619 Henebry, G. M. (2009). Carbon in idle croplands. *Nature,* 457(7233), 1089-1090.
620 https://doi.org/10.1038/4571089a

621 Hess, D., & Tasa, D. (2019). *McKnight's Physical Geography: A Landscape Appreciation.*
622 London: Pearson Education.

623 Horion, S., Prishchepov, A. V., Verbesselt, J., de Beurs, K., Tagesson, T., & Fensholt, R.
624 (2016). Revealing turning points in ecosystem functioning over the Northern Eurasian
625 agricultural frontier. *Global change biology,* 22(8), 2801-2817.
626 https://doi.org/10.1111/gcb.13267

627 Im, A., Lee, E., & He, Y. (2026). Detecting land cover and land use transitions and the
628 associated temperature changes in the East Asian monsoon region. *The Geographical*
629 *Journal*, 192(1), e12590. https://doi.org/10.1111/geoj.12590

630 Ioffe, G., Nefedova, T., & Zaslavsky, I. (2004). From spatial continuity to fragmentation: the
631 case of Russian farming. *Annals of the Association of American Geographers,* 94(4), 913-
632 943. https://doi.org/10.1111/j.1467-8306.2004.00441.x

633 IPCC. (2022). Climate Change 2022: Impacts, Adaptation, and Vulnerability. Contribution of
634 Working Group II to the Sixth Assessment Report of the Intergovernmental Panel on
635 Climate Change [H.-O. Pörtner, D.C. Roberts, M. Tignor, E.S. Poloczanska, K.
636 Mintenbeck, A. Alegría, M. Craig, S. Langsdorf, S. Löschke, V. Möller, A. Okem, B.

637 Rama (eds.)]. Cambridge University Press. Cambridge University Press, Cambridge, UK
638 and New York, NY, USA, 3056 pp. https://doi.org/10.1017/9781009325844

639 Kang, Y., Ozdogan, M., Gao, F., Anderson, M. C., White, W. A., Yang, Y., ... & Erickson, T.
640 A. (2021). A data-driven approach to estimate leaf area index for Landsat images over the
641 contiguous US. Remote Sensing of Environment, 258, 112383.
642 https://doi.org/10.1016/j.rse.2021.112383

643 Kariyeva, J., & van Leeuwen, W. J. (2012). Phenological dynamics of irrigated and natural
644 drylands in Central Asia before and after the USSR collapse. *Agriculture, ecosystems &*
645 *environment*, 162, 77-89. https://doi.org/10.1016/j.agee.2012.08.006

646 Kendall, M. G. (1948). *Rank correlation methods*. London, UK: Griffin.

647 Kraemer, R., Prishchepov, A. V., Müller, D., Kuemmerle, T., Radeloff, V. C., Dara, A., et al.
648 (2015). Long-term agricultural land-cover change and potential for cropland expansion in
649 the former Virgin Lands area of Kazakhstan. *Environmental Research Letters,* 10(5),
650 054012. https://doi.org/10.1088/1748-9326/10/5/054012

651 Kurganova, I., De Gerenyu, V. L., & Kuzyakov, Y. (2015). Large-scale carbon sequestration
652 in post-agrogenic ecosystems in Russia and Kazakhstan. *Catena,* 133, 461-466.
653 https://doi.org/10.1016/j.catena.2015.06.002

654 Lawrence, D. M., Hurtt, G. C., Arneth, A., Brovkin, V., Calvin, K. V., Jones, A. D., et al.
655 (2016). The Land Use Model Intercomparison Project (LUMIP) contribution to CMIP6:
656 Rationale and experimental design. *Geoscientific Model Development,* 9(9), 2973–2998.
657 https://doi.org/10.5194/gmd-9-2973-2016

658 Lawrence, P. J., Feddema, J. J., Bonan, G. B., Meehl, G. A., O'Neill, B. C., Oleson, K. W., et
659 al. (2012). Simulating the biogeochemical and biogeophysical impacts of transient land
660 cover change and wood harvest in the Community Climate System Model (CCSM4) from
661 1850 to 2100. *Journal of Climate,* 25(9), 3071-3095. https://doi.org/10.1175/JCLI-D-11-
662 00256.1

663 Lee, E., He, Y., Zhou, M., & Liang, J. (2015). Potential feedback of recent vegetation
664 changes on summer rainfall in the Sahel. *Physical Geography,* 36(6), 449-470.
665 https://doi.org/10.1080/02723646.2015.1120139

666 Lee, E., Sacks, W. J., Chase, T. N., & Foley, J. A. (2011). Simulated impacts of irrigation on

667 the atmospheric circulation over Asia. *Journal of Geophysical Research: Atmospheres,*
668 116(D8), 1-13. https://doi.org/10.1029/2010JD014740

669 Lejeune, Q., Davin, E. L., Gudmundsson, L., Winckler, J., & Seneviratne, S. I. (2018).
670 Historical deforestation locally increased the intensity of hot days in northern mid-
671 latitudes. Nature Climate Change, 8(5), 386-390. https://doi.org/10.1038/s41558-018-
672 0131-z

673 Li, Z., Chen, Y., Li, W., Deng, H., & Fang, G. (2015). Potential impacts of climate change on
674 vegetation dynamics in Central Asia. *Journal of Geophysical Research: Atmospheres*,
675 120(24), 12345-12356. https://doi.org/10.1002/2015JD023618

676 Lioubimtseva, E., & Henebry, G. M. (2009). Climate and environmental change in arid
677 Central Asia: Impacts, vulnerability, and adaptations. *Journal of Arid Environments,*
678 73(11), 963-977. https://doi.org/10.1016/j.jaridenv.2009.04.022

679 Liu, H., Gong, P., Wang, J., Clinton, N., Bai, Y., & Liang, S. (2020). Annual dynamics of
680 global land cover and its long-term changes from 1982 to 2015. *Earth System Science*
681 *Data*, 12(2), 1217-1243. https://doi.org/10.5194/essd-12-1217-2020

682 Liu, J., Shen, W., & He, Y. (2021). Effects of cropland expansion on temperature extremes in
683 western India from 1982 to 2015. *Land*, 10(5), 489. https://doi.org/10.3390/land10050489

684 Luo, X., Ge, J., Cao, Y., Liu, Y., Yang, L., Wang, S., & Guo, W. (2024). Local and nonlocal
685 biophysical effects of historical land use and land cover changes in CMIP6 models and
686 the intermodel uncertainty. *Earth's Future,* 12(6), e2023EF004220.
687 https://doi.org/10.1029/2023EF004220

688 Lyuri, D. I., Goryachkin, S. V., Karavaeva, N. A., Denisenko, E. A., & Nefedova, T. G.
689 (2010). *Dynamics of agricultural lands of Russia in XX century and postagrogenic*
690 *restoration of vegetation and soils.* Moscow, Russia: GEOS.

691 Löw, F., Fliemann, E., Abdullaev, I., Conrad, C., & Lamers, J. P. (2015). Mapping
692 abandoned agricultural land in Kyzyl-Orda, Kazakhstan using satellite remote sensing.
693 *Applied Geography,* 62, 377-390. https://doi.org/10.1016/j.apgeog.2015.05.009

694 Löw, F., Prishchepov, A. V., Waldner, F., Dubovyk, O., Akramkhanov, A., Biradar, C., et al.
695 (2018). Mapping cropland abandonment in the Aral Sea Basin with MODIS time
696 series. *Remote Sensing,* 10(2), 159. https://doi.org/10.3390/rs10020159

Mahmood, R., Pielke Sr, R. A., Hubbard, K. G., Niyogi, D., Dirmeyer, P. A., McAlpine, C., et al. (2014). Land cover changes and their biogeophysical effects on climate. *International journal of climatology,* 34(4), 929-953. https://doi.org/10.1002/joc.3736

Mann, H. B. (1945). Nonparametric tests against trend. *Econometrica: Journal of the econometric society*, 13(3), 245-259. https://doi.org/10.2307/1907187

Masson-Delmotte, V., et al. (Eds.). (2018). *Global Warming of 1.5 °C: An IPCC Special Report on the impacts of global warming of 1.5 °C above pre-industrial levels and related global greenhouse gas emission pathways, in the context of strengthening the global response to the threat of climate change, sustainable development, and efforts to eradicate poverty.* Cambridge, UK: Cambridge University Press. https://doi.org/10.1017/9781009157940

McCauley, M. (2016). *Khrushchev and the Development of Soviet Agriculture: Virgin Land Program*. London: Palgrave Macmillan.

Meyfroidt, P., Schierhorn, F., Prishchepov, A. V., Müller, D., & Kuemmerle, T. (2016). Drivers, constraints and trade-offs associated with recultivating abandoned cropland in Russia, Ukraine and Kazakhstan. *Global Environmental Change,* 37, 1-15. https://doi.org/10.1016/j.gloenvcha.2016.01.003

Middel, A., Brazel, A. J., Gober, P., Myint, S. W., Chang, H., & Duh, J. (2012). Land cover, climate, and the summer surface energy balance in Phoenix, AZ, and Portland, OR. *International Journal of Climatology,* 32(13), 2020-2032. https://doi.org/10.1002/joc.2408

Middleton, N., & Thomas, D. (Eds.). (1997). *World atlas of desertification*. London: Arnold, Hodder Headline, PLC.

Mirzabaev, A. (2023). *Climate Change in Central Asia: Decarbonization, Energy Transition and Climate Policy.* Cham, Switzerland: Springer.

Morgounov, A., & Trethowan, R. (2008). *Avenues to increase yield potential of short season, high latitude wheat in Northern Kazakhstan and Siberia. In International Symposium on Wheat Yield Potential.* El Batan, Mexico: CIMMYT.

Muñoz-Sabater, J., Dutra, E., Agustí-Panareda, A., Albergel, C., Arduini, G., Balsamo, G., et al. (2021). ERA5-Land: A state-of-the-art global reanalysis dataset for land applications.

Earth system science data, 13(9), 4349-4383. https://doi.org/10.5194/essd-13-4349-2021

Myneni, R. B., & Williams, D. L. (1994). On the relationship between FAPAR and NDVI. Remote sensing of environment, 49(3), 200-211. https://doi.org/10.1016/0034-4257(94)90016-7

National Oceanic and Atmospheric Administration (NOAA), Climate Prediction Center (CPC). (n.d.). Oceanic Niño Index (ONI). NOAA Climate Prediction Center. https://www.cpc.ncep.noaa.gov/products/analysis_monitoring/ensostuff/ONI_v5.php

Olusegun, C. F., & Adeyewa, Z. D. (2013). Spatial and temporal variation of normalized difference vegetation index (NDVI) and rainfall in the north east arid zone of Nigeria. *Atmospheric and Climate Sciences,* 3(4), 421–426. http://dx.doi.org/10.4236/acs.2013.34043

Ortiz-Oliveros, H. B., Avila-Pérez, P., Cruz-González, D., Villalva-Hernández, A., Lara-Almazán, N., Torres-García, I. (2022). Climatic and hydrological variations caused by Land Use/Land Cover changes in the valley of Toluca, Mexico: A rapid assessment. *Sustainable Cities and Society,* 85, 104074. https://doi.org/10.1016/j.scs.2022.104074

Ozdogan, M., Rodell, M., Beaudoing, H. K., & Toll, D. L. (2010). Simulating the Effects of Irrigation over the United States in a Land Surface Model Based on Satellite-Derived Agricultural Data. *Journal of Hydrometeorology,* 11(1), 171–184. https://doi.org/10.1175/2009JHM1116.1

Park, H., & Jeong, S. (2021). Leaf area index in Earth system models: how the key variable of vegetation seasonality works in climate projections. *Environmental Research Letters* 16(3), 034027. https://doi.org/10.1088/1748-9326/abe2cf

Perugini, L., Caporaso, L., Marconi, S., Cescatti, A., Quesada, B., de Noblet-Ducoudré, N., ... & Arneth, A. (2017). Biophysical effects on temperature and precipitation due to land cover change. Environmental Research Letters, 12(5), 053002. https://doi.org/10.1088/1748-9326/aa6b3f

Pielke Sr, R. A. (2005). Land use and climate change. *Science,* 310(5754), 1625-1626. https://doi.org/10.1126/science.1120529

Pinzon, J. E., Pak, E. W., Tucker, C. J., Bhatt, U. S., Frost, G. V., & Macander, M. J. (2023). Global Vegetation Greenness (NDVI) from AVHRR GIMMS-3G+, 1981-2022 (Version

1) [Dateset]. ORNL Distributed Active Archive Center. https://doi.org/10.3334/ORNLDAAC/2187

Pitman, A. J., de Noblet-Ducoudré, N., Cruz, F. T., Davin, E. L., Bonan, G. B., Brovkin, V., ... & Voldoire, A. (2009). Uncertainties in climate responses to past land cover change: First results from the LUCID intercomparison study. Geophysical Research Letters, 36(14). https://doi.org/10.1029/2009GL039076

Pongratz, J., Schwingshackl, C., Bultan, S., Obermeier, W., Havermann, F., & Guo, S. (2021). Land use effects on climate: current state, recent progress, and emerging topics. Current Climate Change Reports, 7(4), 99-120. https://doi.org/10.1007/s40641-021-00178-y

Prishchepov, A. V., Radeloff, V. C., Baumann, M., Kuemmerle, T., & Müller, D. (2012). Effects of institutional changes on land use: agricultural land abandonment during the transition from state-command to market-driven economies in post-Soviet Eastern Europe. *Environmental Research Letters,* 7(2), 024021. https://doi.org/10.1088/1748-9326/7/2/024021

Pörtner, H.-O., et al. (Eds.). (2022). *Climate Change 2022: Impacts, Adaptation and Vulnerability. Contribution of Working Group II to the Sixth Assessment Report of the Intergovernmental Panel on Climate Change.* Cambridge, UK: Cambridge University Press. https://doi.org/10.1017/9781009325844

Qing, Y., Wang, S., AghaKouchak, A., & Gentine, P. (2025). Delayed formation of Arctic snow cover in response to wildland fires in a warming climate. *Nature climate change*, 15, 1091–1098. https://doi.org/10.1038/s41558-025-02443-6

Rajagopalan, B., & Molnar, P. (2013). Signatures of Tibetan Plateau heating on Indian summer monsoon rainfall variability. *Journal of Geophysical Research: Atmospheres*, 118(3), 1170-1178. https://doi.org/10.1002/jgrd.50124

Saiko, T. A., & Zonn, I. S. (2000). Irrigation expansion and dynamics of desertification in the Circum-Aral region of Central Asia. *Applied Geography*, 20(4), 349-367. https://doi.org/10.1016/S0143-6228(00)00014-X

Schmidt, M., Klein, D., Conrad, C., Dech, S., & Paeth, H. (2014). On the relationship between vegetation and climate in tropical and northern Africa. *Theoretical and Applied*

787 *Climatology,* 115, 341–353. https://doi.org/10.1007/s00704-013-0900-6

788 Sen, P. K. (1968). Estimates of the regression coefficient based on Kendall's tau. *Journal of*
789 *the American statistical association,* 63(324), 1379-1389.
790 https://doi.org/10.1080/01621459.1968.10480934

791 Seneviratne, S. I., Lüthi, D., Litschi, M., & Schär, C. (2006). Land–atmosphere coupling and
792 climate change in Europe. Nature, 443(7108), 205-209.
793 https://doi.org/10.1038/nature05095

794 Siderius, C., Hellegers, P. J. G. J., Mishra, A., van Ierland, E. C., & Kabat, P. (2014).
795 Sensitivity of the agroecosystem in the Ganges basin to inter-annual rainfall variability
796 and associated changes in land use. *International Journal of Climatology*, 34(10), 3066-
797 3077. https://doi.org/10.1002/joc.3894

798 Streiner, D. L. (2005). Finding our way: an introduction to path analysis. *The Canadian*
799 *Journal of Psychiatry*, 50(2), 115–122. https://doi.org/10.1177/070674370505000207

800 Sugihara, G., May, R., Ye, H., Hsieh, C. H., Deyle, E., Fogarty, M., & Munch, S. (2012).
801 Detecting causality in complex ecosystems. *science*, 338(6106), 496-500.
802 https://doi.org/10.1126/science.1227079

803 Takens, F. (1981). Detecting strange attractors in turbulence. Dynamical systems and
804 turbulence, Warwick 1980, 366-381. https://doi.org/10.1007/BFb0091924

805 Turner, B. L., Lambin, E. F., & Reenberg, A. (2007). The emergence of land change science
806 for global environmental change and sustainability. *Proceedings of the National Academy*
807 *of Sciences,* 104(52), 20666-20671. https://doi.org/10.1073/pnas.0704119104

808 Vakulchuk, R., Daloz, A. S., Overland, I., Sagbakken, H. F., & Standal, K. (2023). A void in
809 Central Asia research: climate change. *Central Asian Survey*, 42(1), 1–20.
810 https://doi.org/10.1080/02634937.2022.2059447

811 Wei, W., Zhang, R., Wen, M., & Yang, S. (2017). Relationship between the Asian westerly
812 jet stream and summer rainfall over central Asia and North China: Roles of the Indian
813 monsoon and the South Asian high. *Journal of Climate,* 30(2), 537-552.
814 https://doi.org/10.1175/JCLI-D-15-0814.1

815 Xian, G. Z., Loveland, T., Munson, S. M., Vogelmann, J. E., Zeng, X., & Homer, C. J.
816 (2020). Climate sensitivity to decadal land cover and land use change across the

conterminous United States. *Global and Planetary Change,* 192, 103262. https://doi.org/10.1016/j.gloplacha.2020.103262

Xu, X., Riley, W. J., Koven, C. D., Jia, G., & Zhang, X. (2020). Earlier leaf-out warms air in the north. *Nature Climate Change*, 10(4), 370-375. https://doi.org/10.1038/s41558-020-0713-4

Xu, Y., Yang, J., & Chen, Y. (2016). NDVI-based vegetation responses to climate change in an arid area of China. *Theoretical and Applied Climatology,* 126(1), 213-222. https://doi.org/10.1007/s00704-015-1572-1

Yadav, S. K., Lee, E., & He, Y. (2022). Positive associations of vegetation with temperature over the alpine grasslands in the western Tibetan Plateau during May. *Earth Interactions,* 26(1), 94-111. https://doi.org/10.1175/EI-D-21-0017.1

Ye, H., Deyle, E. R., Gilarranz, L. J., & Sugihara, G. (2015). Distinguishing time-delayed causal interactions using convergent cross mapping. Scientific reports, 5(1), 14750. https://doi.org/10.1038/srep14750

Yuan, X., Wang, W., Cui, J., Meng, F., Kurban, A., & De Maeyer, P. (2017). Vegetation changes and land surface feedbacks drive shifts in local temperatures over Central Asia. *Scientific Reports,* 7, 3287. https://doi.org/10.1038/s41598-017-03432-2

Zhu, Z., Piao, S., Myneni, R. B., Huang, M., Zeng, Z., Canadell, J. G., ... & Zeng, N. (2016). Greening of the Earth and its drivers. *Nature climate change*, 6(8), 791-795. https://doi.org/10.1038/nclimate3004

Table and Figures

Table 1. Granger-causality test of JJA surface climate variables (2m temperature, surface latent heat flux, surface sensible heat flux, and 2m specific humidity) with (a)–(b) NDVI and (c)–(d) other climate variables. *, **, and *** indicate statistical significance at the 10% level, 5% level, and 1% level, respectively.

(a)

Cause	Model	Residual df	df	F-statistics	*p*-value	Result
NDVI	Unrestricted	28				2m temperature
	Restricted	29	1	2.9725	0.09572*	
NDVI	Unrestricted	28				latent heat flux
	Restricted	29	1	4.1062	0.05235*	
NDVI	Unrestricted	28				sensible heat flux
	Restricted	29	1	0.7633	0.3897	
NDVI	Unrestricted	28				2m specific humidity
	Restricted	29	1	9.5922	0.004411***	

(b)

Cause	Model	Residual df	df	F-statistics	*p*-value	Result
2m temperature	Unrestricted	28				NDVI
	Restricted	29	1	0.0241	0.8777	
latent heat flux	Unrestricted	28				NDVI
	Restricted	29	1	0.234	0.6324	
sensible heat flux	Unrestricted	28				NDVI
	Restricted	29	1	0.0151	0.903	
2m specific humidity	Unrestricted	28				NDVI
	Restricted	29	1	0.0413	0.8405	

(c)

Cause	Model	Residual df	df	F-statistics	*p*-value	Result
latent heat flux	Unrestricted	28				2m temperature
	Restricted	29	1	3.1237	0.08806*	
latent heat flux	Unrestricted	28				sensible heat flux
	Restricted	29	1	0.8037	0.3776	
latent heat flux	Unrestricted	28				2m specific humidity
	Restricted	29	1	3.8028	0.06124*	

(d)

Cause	Model	Residual df	df	F-statistics	*p*-value	Result
2m temperature	Unrestricted	28				latent heat flux
	Restricted	29	1	2.1549	0.1533	
sensible heat flux	Unrestricted	28				latent heat flux
	Restricted	29	1	1.7442	0.1973	
2m specific humidity	Unrestricted	28				latent heat flux
	Restricted	29	1	2.0786	0.1605	

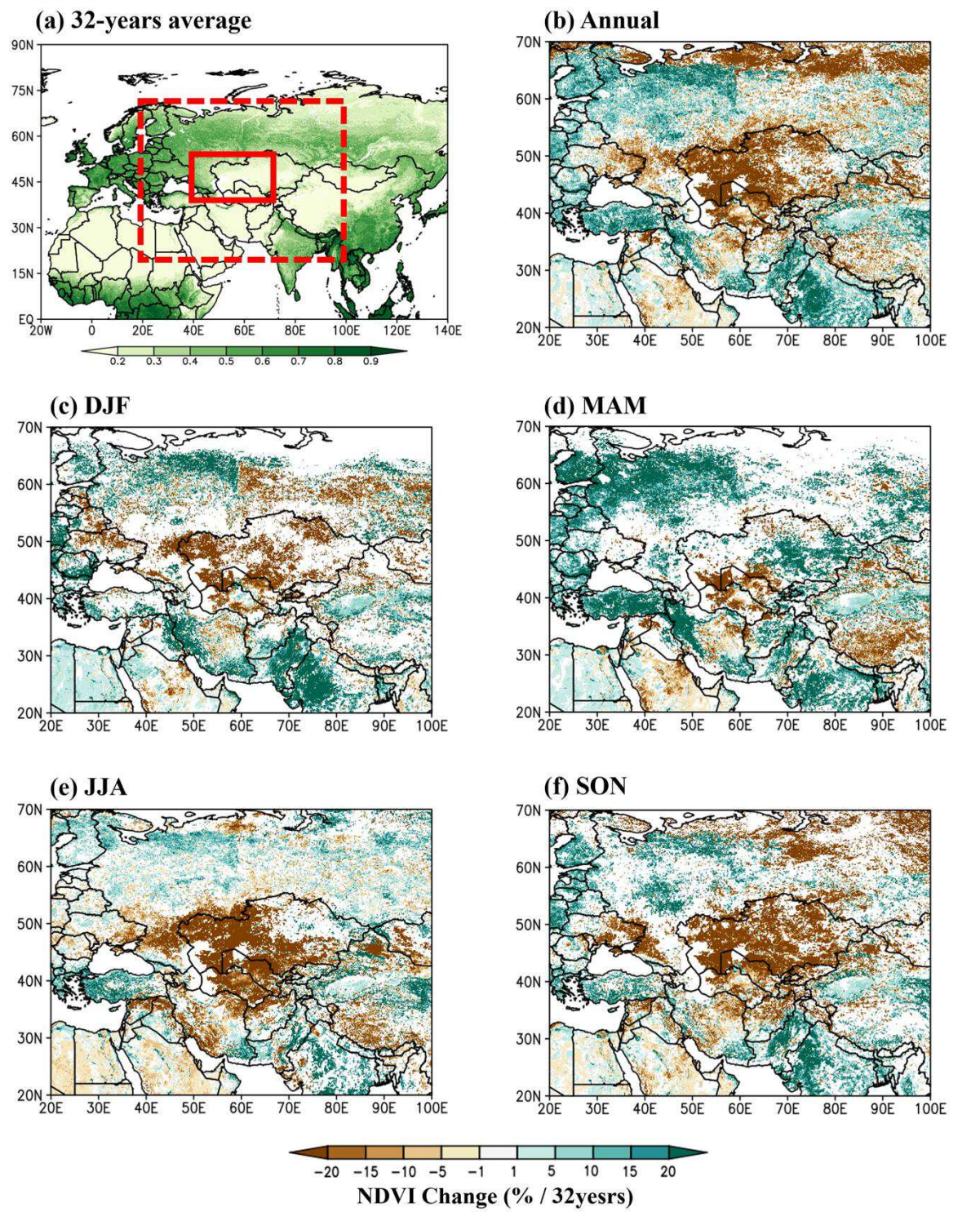


Figure 1. Climatological means and trends of vegetation from 1991 to 2022 with (a) annual average of NDVI, and the percentage of NDVI change to the mean for (b) annual, (c) DJF, (d) MAM, (e) JJA, and (f) SON. The red dashed box in (a) indicates Central Asia and its surrounding regions (20–70°N, 20–100°E), and the solid box represents our study regions (European Russia and northwestern Kazakhstan) (40–52°N, 40–70°E). Only statistically significant grids are shaded at the 5% level in (b)–(f).

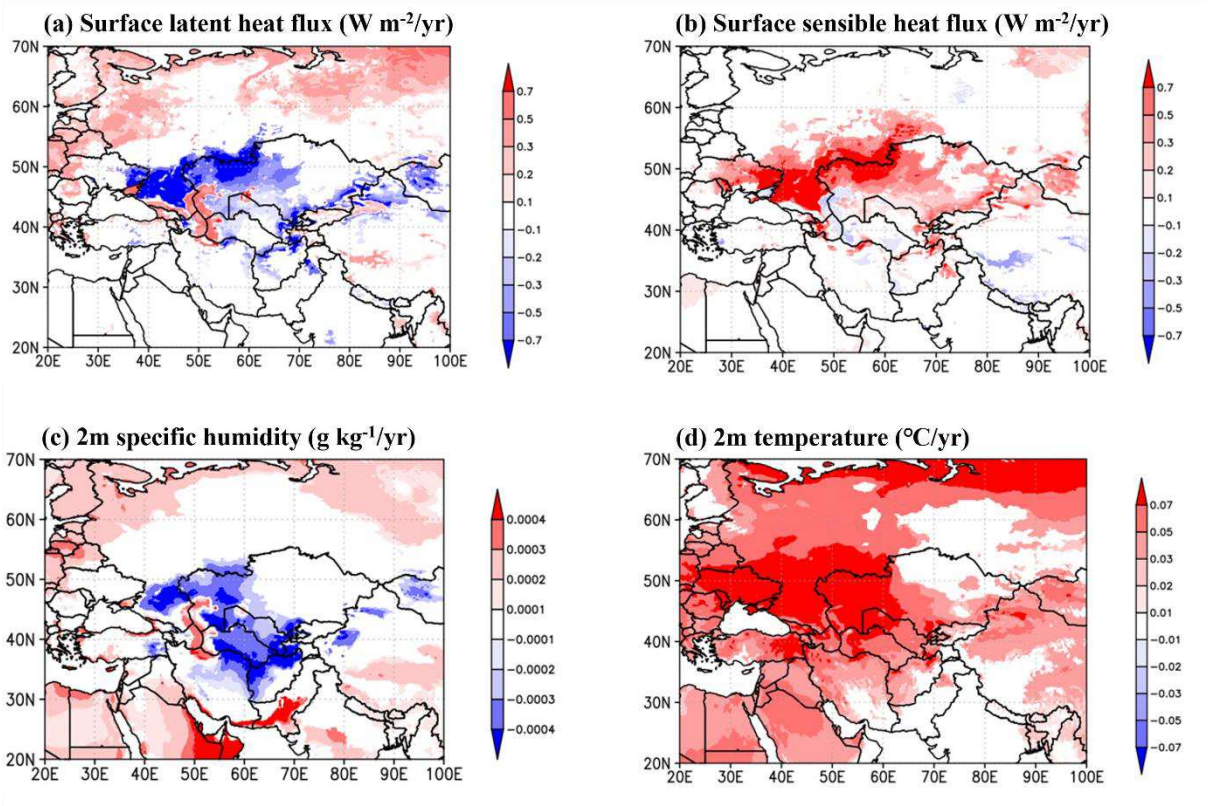
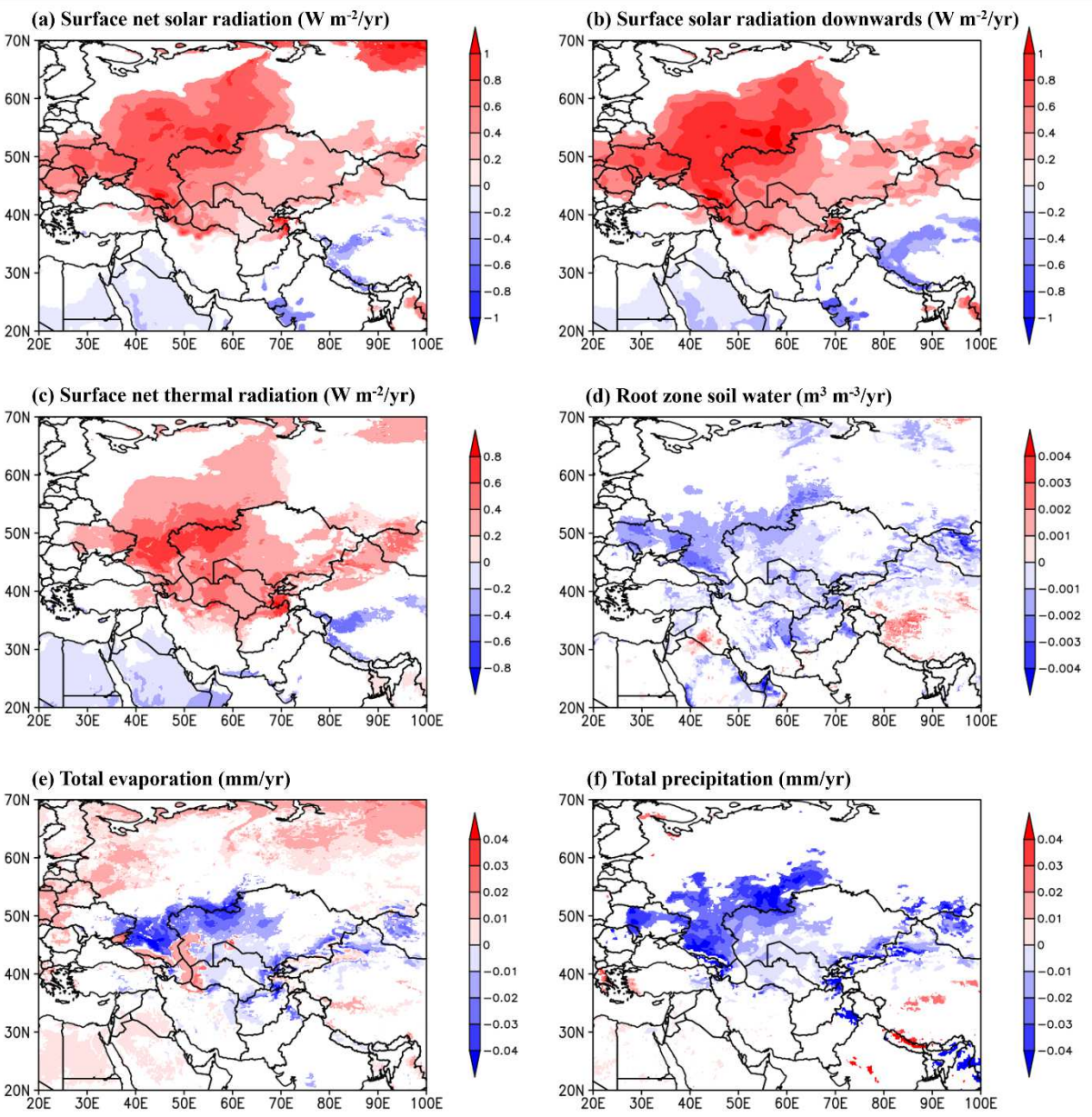


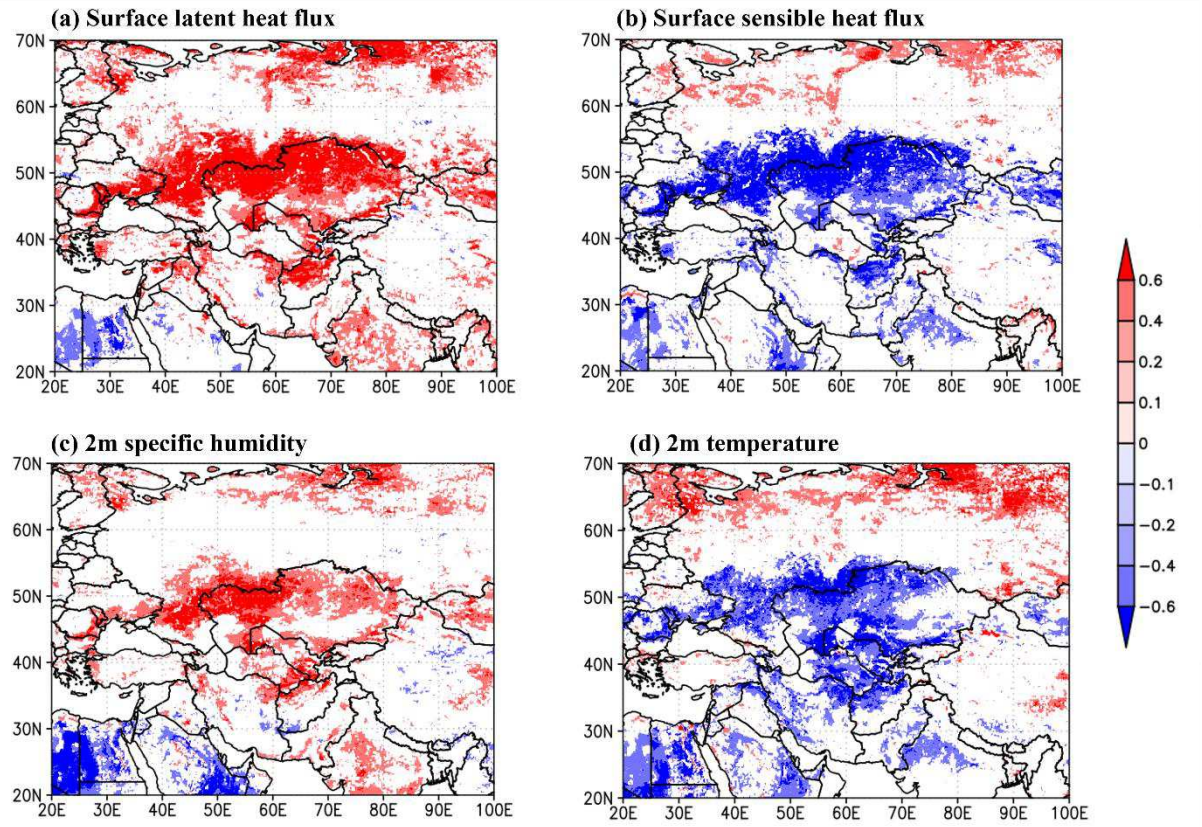
Figure 2. Linear regression trends of surface climate variables of (a) surface latent heat flux (W m^{-2} per year), (b) surface sensible heat flux (W m^{-2} per year), (c) 2m specific humidity (g kg^{-1} per year), and (d) 2m temperature (°C per year) during JJA from 1991 to 2022. Only statistically significant grids are shaded at the 5% level.



862

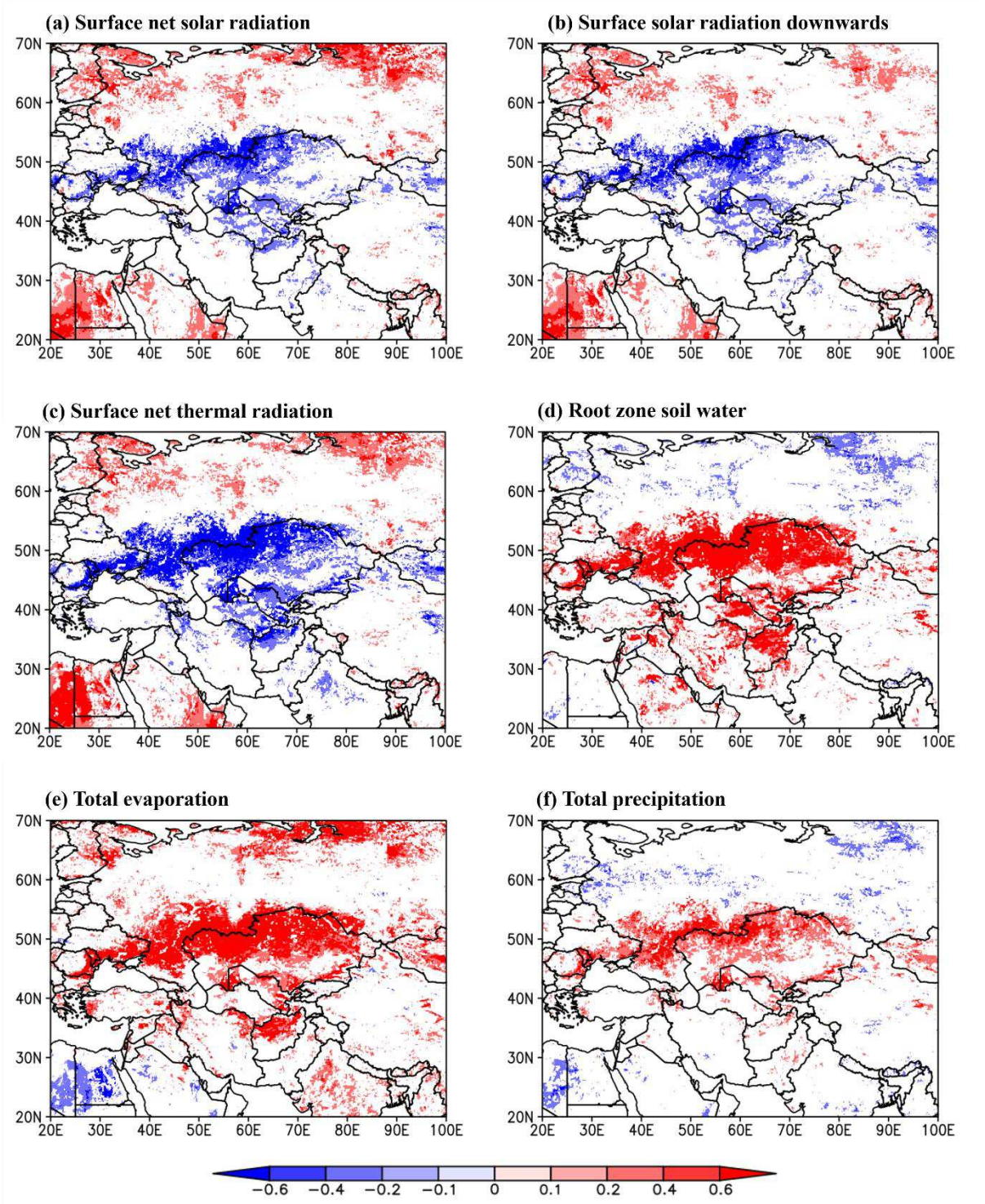
863 **Figure 3.** Same as in Figure 2, but with (a) surface net solar radiation (W m^{-2} per year), (b)
864 surface solar radiation downwards (W m^{-2} per year), (c) surface net thermal radiation (W m^{-2}
865 per year), (d) root zone soil water (m^3 m^{-3} per year), (e) total evaporation (mm per year), and
866 (f) total precipitation (mm per year)

867



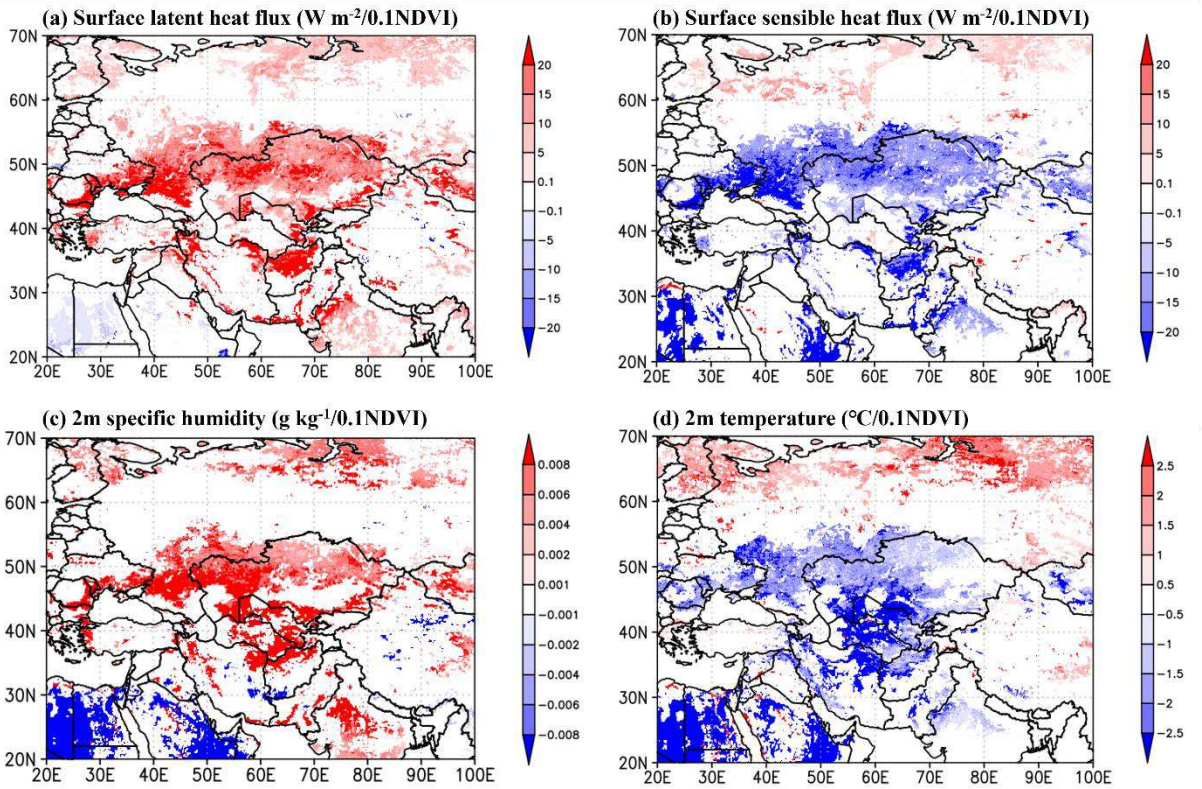
868

869 **Figure 4.** Correlation coefficients of NDVI with (a) surface latent heat flux, (b) surface sensible
870 heat flux, (c) 2m specific humidity, and (d) 2m temperature during JJA from 1991 to 2022 at
871 each grid point. Only statistically significant grids are represented at the 5% level.



872

873 **Figure 5.** Same as in Figure 4, but with (a) surface net solar radiation (W m^{-2} per year), (b)
874 surface solar radiation downwards (W m^{-2} per year), (c) surface net thermal radiation (W m^{-2}
875 per year), (d) root zone soil water (m^3 m^{-3} per year), (e) total evaporation (mm per year), and
876 (f) total precipitation (mm per year)



877

878 **Figure 6.** Linear regression slopes of (a) surface latent heat flux (W m^{-2} per 0.1 NDVI), (b)
879 surface sensible heat flux (W m^{-2} per 0.1 NDVI), (c) 2m specific humidity (g kg^{-1} per 0.1
880 NDVI), and (d) 2m temperature (°C per 0.1 NDVI) with NDVI during JJA from 1991 to 2022
881 at each grid cell. Only statistically significant grids are represented at the 5% level.

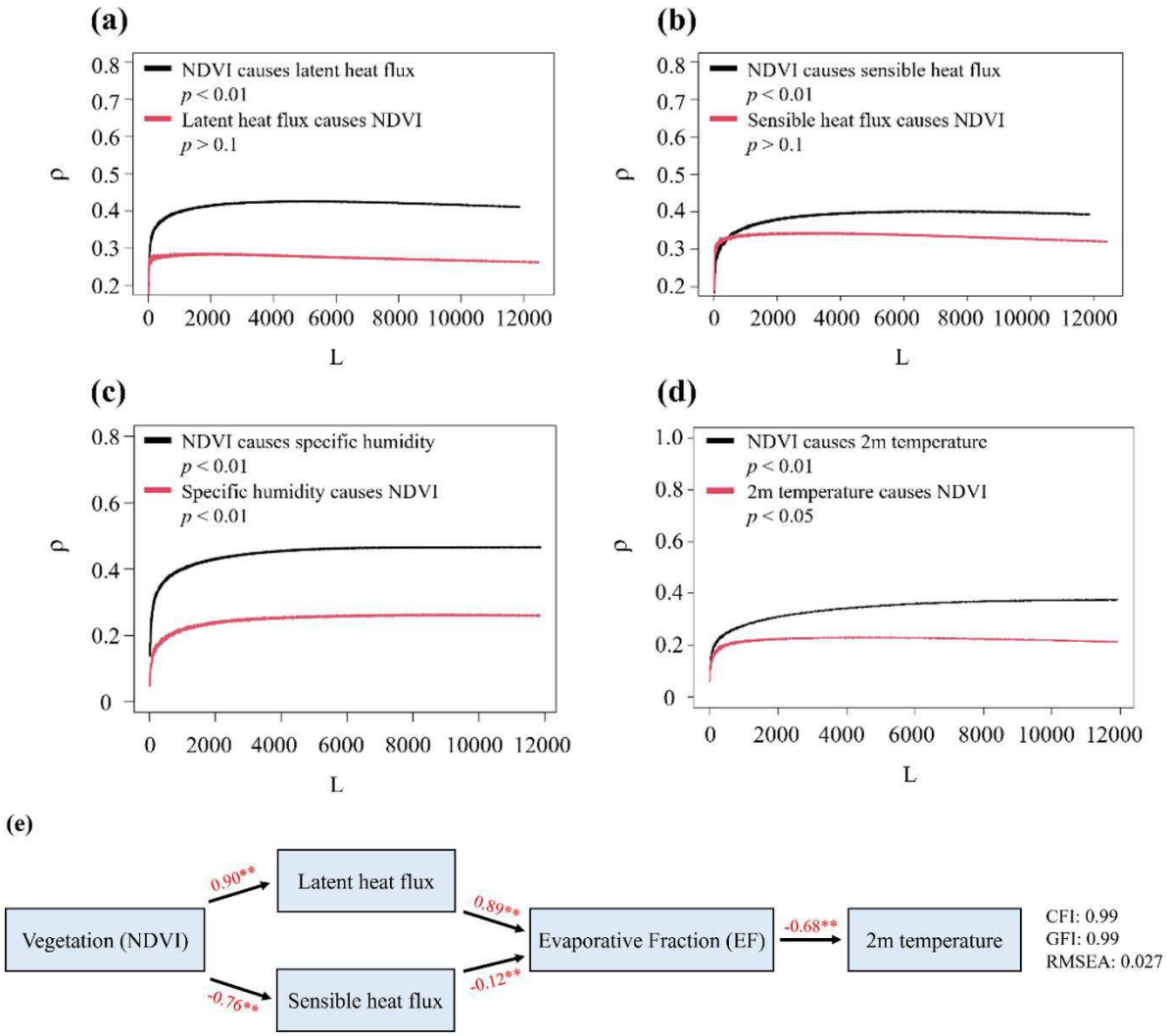


Figure 7. Causal relationships between JJA vegetation and surface climate variables (latent heat flux, sensible heat flux, 2m specific humidity, and 2m temperature) by CCM and SEM. Upper panel represents the CCM results between NDVI and (a) latent heat flux, (b) sensible heat flux, (c) 2m specific humidity, and (d) 2m temperature. (e) Lower panel shows the SEM illustrating the causal relationship among these variables. Standardized path coefficients are shown along arrows; ** indicates statistical significance at the 1% level. CFI, GFI, and RMSEA indicate comparative fit index, goodness of fit index, and root mean square error of approximation, respectively.

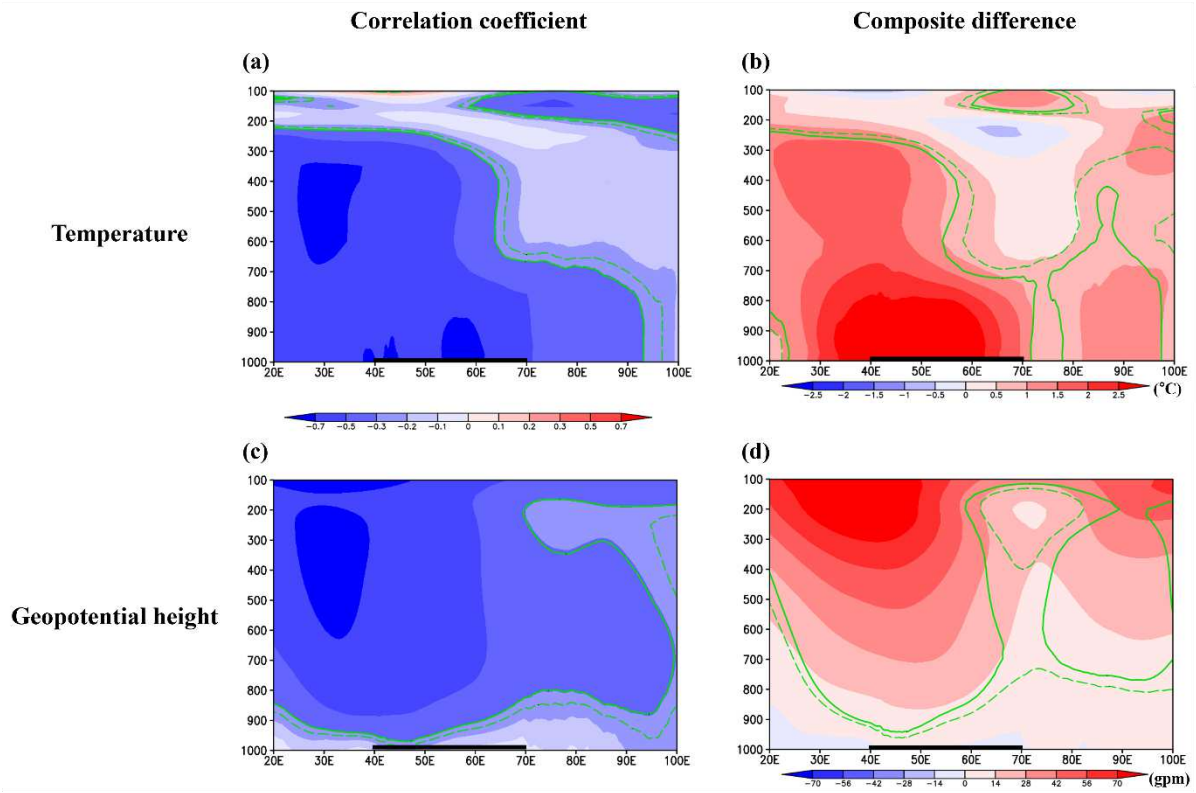


Figure 8. Vertical cross sections of (a), (c) correlation coefficients of JJA tropospheric variables (temperature and geopotential height) with JJA NDVI time series, area averaged over European Russia and northwestern Kazakhstan (40–52°N and 40–70°E); and (b), (d) composite differences of the JJA tropospheric variables between the years with low and high NDVI. The years in the bottom 20% of the lowest NDVI values were 2021, 2020, 2019, 2018, 2012, and 2010, and those in the top 20% of the highest NDVI values were 1993, 1997, 1992, 2000, 1994, and 2003. Black bars indicate the longitude range of the study region (40-70°E). Statistically significant areas at the 10% and 5% levels are contoured by dashed and solid lines, respectively.

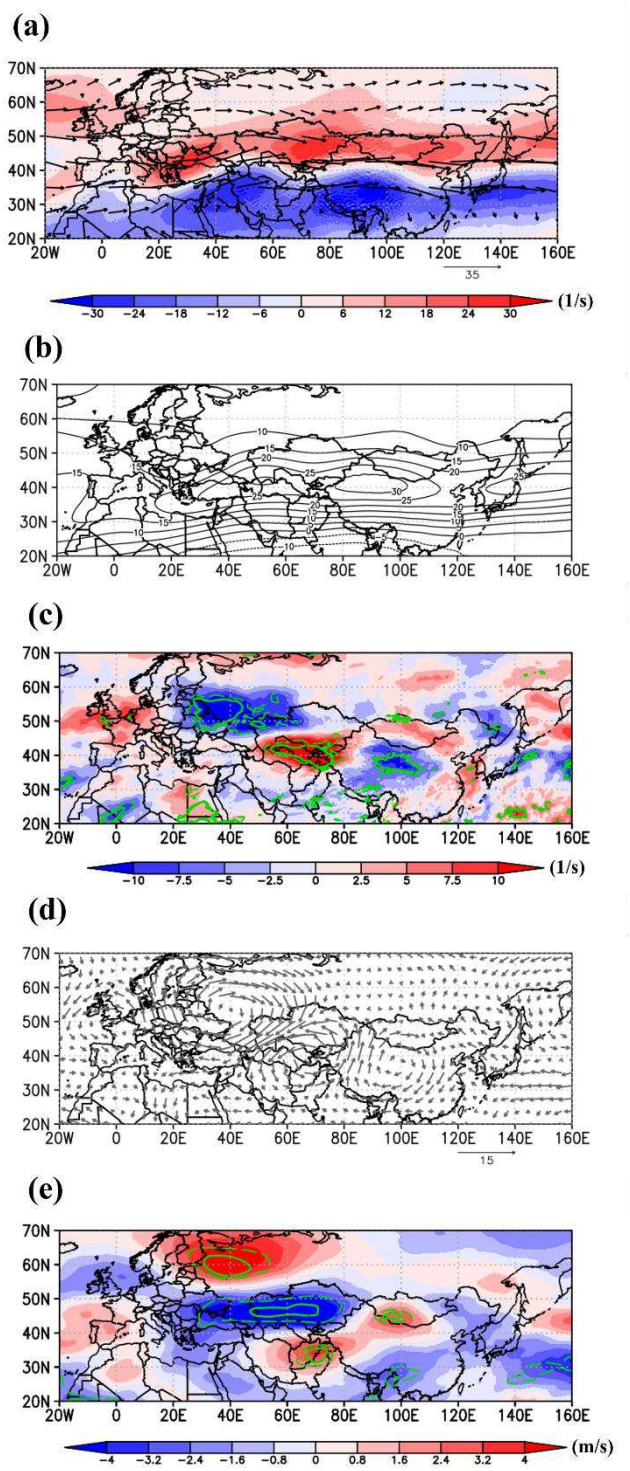


Figure 9. 32-year JJA averages of (a) vorticity with wind vectors and (b) *u*-wind at 200 hPa. Composite differences for (c) vorticity (1 s^{-1}), (d) wind vectors (m s^{-1}), and (e) *u*-wind (m s^{-1}) at 200 hPa. The years in the top 20% of the highest NDVI values were 1993, 1997, 1992, 2000, 1994, and 2003, and those in the bottom 20% of the lowest NDVI values were 2021, 2020, 2019, 2018, 2012, and 2010. Statistically significant areas at the 10% and 5% levels are contoured by dashed and solid lines, respectively.

Supplementary Files

This is a list of supplementary files associated with this preprint. Click to download.

- SupplementaryInformation.docx